Low misfit systems as tools for understanding dislocation relaxation mechanisms in semiconducting heteroepitaxial films

2002 J. Phys.: Condens. Matter 14 13255

(http://iopscience.iop.org/0953-8984/14/48/376)

INSTITUTE OF PHYSICS PUBLISHING JOURNAL OF PHYSICS: CONDENSED MATTER

J. Phys.: Condens. Matter **14** (2002) 13255–13267 PII: S0953-8984(02)53997-7

Low misfit systems as tools for understanding dislocation relaxation mechanisms in semiconducting heteroepitaxial films

B Pichaud[1,3], N Burle[1], M Putero-Vuaroqueaux[1,2] and C Curtil[1]

[1] Laboratoire TECSEN UMR 6122, Université Aix-Marseille III, 13397 Marseille Cedex 20, France
[2] L2MP UMR 6137, Université Aix-Marseille III, 13397 Marseille Cedex 20, France

Received 27 September 2002
Published 22 November 2002
Online at stacks.iop.org/JPhysCM/14/13255

Abstract

In low misfit systems ($m < 1\%$) the elemental dislocation mechanisms can be observed over large areas; this provides information on the ways the relaxation proceeds in higher misfit heteroepitaxial systems where large dislocation densities are rapidly generated and in which these mechanisms are not easy to discover among dislocation configurations resulting from this highly deformed state. Heteroepitaxial (GaAs/Ge, SiGe/Si, GaInAs/GaAs) and homoepitaxial (Si/Si(As)) systems were considered in which the relaxation steps were studied: nucleation, and dislocation multiplication.

The Matthews mechanism for misfit dislocation nucleation was observed in a very metastable situation. This was ascribed to thermal activation of the source length rather than to the processes reported in the literature.

During the development of dislocations several types of interaction occurred leading to threading segments. The very frequent occurrence of cross-slip and multiple cross-slip events allows the relaxation to proceed in spite of blocking interactions. This unexpected easy cross-slip can be related to a shrinkage of the fault ribbon close to the surface due to image forces.

1. Introduction

Strained layer semiconductor heterostructures have been established as an important part of the fabrication of electronic and optoelectronic devices. A strained layer can store a very high elastic energy proportional to the square of the misfit m (relative difference between the film and substrate lattice parameters) and to its thickness t, until it becomes more favourable to relax this strain energy. Among all the relaxation processes, we will consider in this paper only the dislocation induced relaxation mechanisms which involve a critical thickness t_c first predicted by Frank and van de Merwe [1], above which interfacial dislocation arrays will

[3] Author to whom any correspondence should be addressed.

reduce the energy of the system. Another approach to this problem, strictly equivalent, is the one proposed by Matthews and Blakeslee [2] who considered the development of interfacial dislocations from pre-existing threading segments driven by the misfit stress against their line tension. This plastic relaxation is commonly encountered in the usual crystal growth and processing conditions for epilayer/substrate systems with a misfit below 3%.

In this domain a large number of systems have been studied based on the association of elemental semiconductors and their alloys, the III–V and II–VI compounds and their alloys. Examination of experimental results reveals that generally the transition between the strained unrelaxed state and the (at least partially) relaxed one occurs at a thickness larger than the one predicted by the equilibrium theory and that the discrepancy is higher for lower misfit and temperature. Several kinetic models [3–8] have been proposed to account for this; they are based on the existence of energy barriers involved in the formation, motion and multiplication of misfit dislocations (MDs). Generally these models bring closer the theoretical and experimental critical thickness, but there are still unsolved questions on the mechanisms involved in the film relaxation. The transmission electron microscopy (TEM) technique allows us, in principle, to observe these mechanisms, but as it is mainly adapted to high misfit dislocation densities, that is to high misfit systems, the elemental mechanisms are not easy to identify among complex dislocation configurations resulting from high strains. Additionally, it seems that the observed mechanisms (at least some of them) are strongly dependent on the system itself.

In this paper, rather than developing another discussion of these problems, which indeed should involve a global view of the deformation process, we have chosen to use information on MD behaviour in low mismatch systems which can be use as model systems to better understand some features of dislocation induced relaxation processes. In these systems ($m < 0.1\%$) the relaxation is very progressive; a pseudomorphic layer can be grown with thicknesses far beyond the critical thickness resulting in a high metastability; the dislocation density is very low allowing elemental mechanisms to be observed over large interfacial areas (typically 1 cm $\times$ 1 cm) using x-ray topography (either in transmission or reflection setting), a method specially well adapted to low dislocation densities. Here, among all the deformation steps occurring during the plastic relaxation, we will consider the activation of the very first MDs and the strong metastability of these systems; we will also discuss the frequent cross-slip events observed during the development of the MDs and their consequences for the completeness of the relaxation.

2. Experiments and results

MDs were analysed by transmission and reflection XRT, which allows us to detect individual MDs and to characterize them fully by determining their Burgers vectors. Transmission topographs were obtained using the Lang setting and a rotating-Ag-anode generator, and reflection topographs with the Berg–Barrett setting and Cu Kα radiation. Strain relaxation was measured by high resolution x-ray diffraction using a four-circle goniometer and Cu Kα radiation.

Several homo- and heteroepitaxial low misfit systems were studied which are reported in table 1 with some characteristic parameters and growth techniques.

2.1. Metastability

In all the systems reported in table 1 a high metastability of the films was observed confirming that the Matthews critical thickness should be considered as a necessary but not sufficient condition for MD development. For a given system, the measured critical thickness is higher

Table 1. Information concerning the different systems. CSVT stands for close-spaced vapour transport, MBE for molecular beam epitaxy and CVD for chemical vapour deposition. * for (001) oriented interfaces; § for (111) oriented.

Film/substrate	Alloy conc.	Misfit	Film thickness (μm)	Critical thickness (μm)	Growth method	Additional information
GaAs/Ge*		-7.2×10^{-4}	0.14–4	0.24	CSVT—750 °C	Cooling rates 5 °C min^{-1} and 50 °C min^{-1}
$Si_{1-x}Ge_x$/Si*	$3 < x < 6.8\%$	1.2×10^{-3} to 2.9×10^{-3}	0.2–0.7	0.12–0.05	MBE—550 °C to 750 °C	Substrate containing disloc. $\sim 10^3$ cm cm^{-3}
$Ga_{1-x}In_x$/GaAs*	$0.7 < x < 1.2\%$	5×10^{-4} to 8.6×10^{-4}	0.7–1.6	0.19–0.36	MBE—350 °C	
Si/Si(As doped)§ [As] $= 2 \times 10^{-19}$ at. cm^3		$\sim 10^{-4}$	20–100	2	CVD— >1000 °C	

for lower misfit and growth temperature, as already reported, but there are also influences of other growth parameters such as the growth method, the growth rate and the cooling rate. Let us consider the former in the case of the GaAs/Ge system.

Figure 1(a) shows the dislocation configurations that can be observed at the very first stage of the relaxation. This 'hairpin' configuration was shown to consist of a sharp straight part lying at the interface (i.e. the MD labelled I in figure 1) which was nucleated from a threading dislocation corresponding to the blurry curved part located in the substrate (labelled S in figure 1) [9]. This configuration is very close to the one proposed by Matthews and Blakeslee [2] which was used to calculate a critical film thickness t_c for the onset of the relaxation, but here the film thickness 1.2 μm is far above the critical one (table 1). Further increasing the thickness yields crossed grid patterns similar to the one shown in figure1(b). As already noted the experimental thickness corresponding to the onset of the relaxation depends on the cooling rate after the film growth:

(i) in fast cooled samples (50 °C min^{-1}) the very first MDs are observed above a thickness of 1.2 μm;
(ii) in the case of slow cooling (5 °C min^{-1}) these MDs are observed above a thickness of 0.8 μm.

The influence of the cooling rate might be explained either by stress variations due to misfit variations with temperature, which may have drastic effects on relaxation [10], or by the kinetics of gliding dislocations at constant stress. In the case of GaAs/Ge samples, the values of the GaAs and Ge lattice parameters found in the literature and their variations with temperature are not sufficiently accurate to be sure of the misfit evolution during cooling. To check if the cooling effect could not be due to misfit variations during cooling, coupled with a thermal activation of the dislocation velocity, we measured this misfit evolution between room temperature and 450 °C in a furnace directly mounted on a Berg–Barrett setting. (The samples were not annealed at higher temperature to avoid As loss.) These measurements were performed on totally unrelaxed GaAs/Ge samples and we verified that they remained

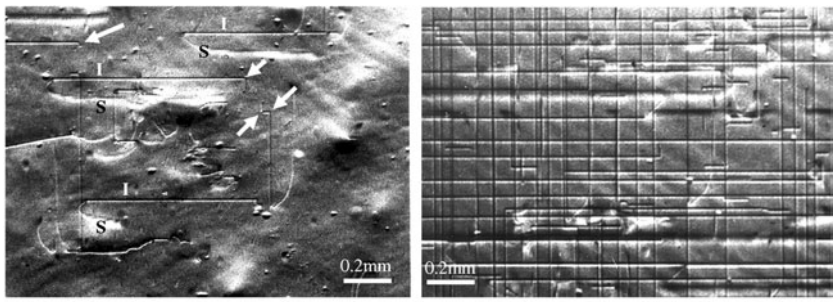

Figure 1. (a) Hairpin dislocations at the very first stage of the plastic relaxation, thickness 1.2 μm, fast cooling, (220) transmission topograph. (b) Cross-hatched MD, thickness 2 μm, fast cooling, (220) transmission topograph.

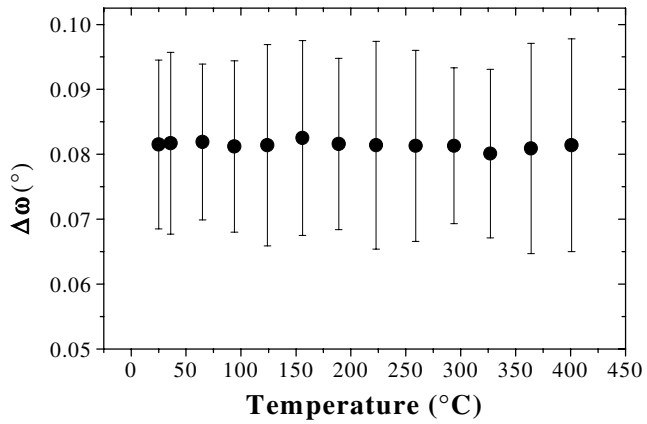

Figure 2. Angular differences $\Delta\omega$ between the (224) reflections of the film (GaAs) and the substrate (Ge) as a function of temperature.

unrelaxed afterwards. The angular distance between the rocking curves from the substrate and the film (asymmetric 224 reflections) was found to be constant (figure 2): therefore the misfit is constant with temperature (<5% variation).

Slightly above 0.8 or 1.2 μm, depending on the cooling rate (slow or fast), we observed some blocking interactions between an emerging part and a long MD dislocation already developed in the film. Figure 3 is a reflection topograph of the layer; the blocking situation is assumed from the corresponding transmission image and the Burgers vector identification. This is the situation proposed by Freund [11] as a mechanism that can delay the relaxation depending on whether the actual film thickness is close to t_c or larger. In our case this interaction often gave a blocking situation even when the film thickness was far above t_c.

Finally we tried to obtain further threading dislocation movement by heating the samples to 430 °C for several days. Many dislocations remained immobile. A few exhibit very limited displacements of the threading part. The corresponding dislocation velocities were estimated to be around 10^{-8} cm s^{-1}, which is very small as compared to those measured in bulk GaAs at this temperature (10^{-5}–10^{-3} cm s^{-1} at 10 MPa and 400 °C [12]).

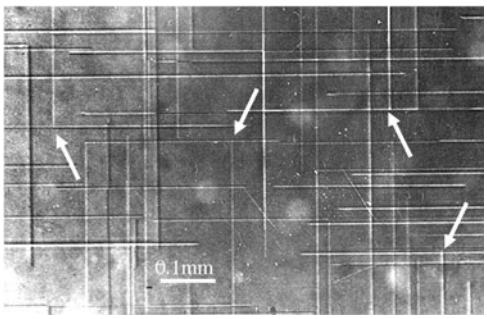

Figure 3. Blocking interactions (arrows) between a threading segment and an MD already developed. (224) reflection from the layer.

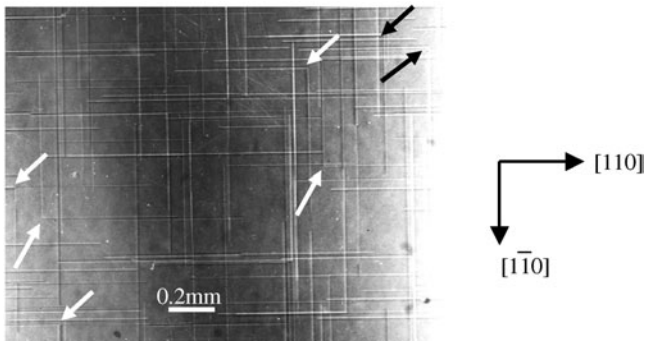

Figure 4. Cross-slip events in the {111} planes in a $Si_{0.97}Ge_{0.03}$/Si sample. Reflection topograph (224).

2.2. Dislocation cross-slip

Figure 4 shows an x-ray image obtained on $Si_{1-x}Ge_x$/Si (with $x = 0.03$) samples, in which MDs have started to develop along the two ⟨110⟩ interface directions with the usual $(a/2)\langle 110\rangle\{111\}$ glide systems. In addition, in this figure as well as in figure 1, cross-slip events from one {111} to another can be identified by a 90° change in the interfacial dislocation direction (arrows). In the case of GaAs/Ge (figure 1) multiple cross-slip events occur as well at the very early stage of the MD development, without any visible interaction which could favour this process (arrows). As reported in section 2.1 the development of the MDs occurs only by moving the emerging segment at the end of the straight part opposite to the curved part. Thus the 90° corners can only be related to a change in glide plane and not to the interaction between two intersecting MDs or to the nucleation of both arms from the corner. In these cases we would observe corners terminated by curved TDs on both sides or abruptly instead of only one arm of the corner terminated by a curved TD as in figure 1(a).

In addition, in several GaAs layers we have observed cross-slip traces which were not parallel to ⟨110⟩ interface directions. Figure 5 demonstrates that cross-slip traces along ⟨100⟩ and ⟨310⟩ directions can occur; these uncommon slip traces correspond respectively to {101} and {131} glide planes. However, the image reveals (figure 5) that the MD dislocation does not move over very long distances in these uncommon glide systems; another cross-slip event allows the MD to return in the {111} glide plane. These observations illustrate the easy occurrence of multiple cross-slip events of MDs at low stress level at the very first stage of

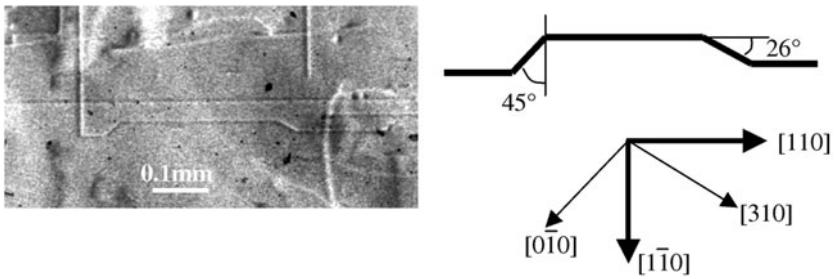

Figure 5. Unusual slip traces and cross-slip events. The slip traces are along [010] and [310] directions indicating cross-slip in {110} and {131} planes. Transmission topograph reflection (220).

the film relaxation process, whereas this mechanism is usually consider to occur at high stress level in bulk materials.

3. Discussion

3.1. Metastability

In the case of the GaAs/Ge system, the films were grown at a rather high temperature, 750 °C; as the thermally activated yielding regime ends just below this temperature [13], the dislocation velocities do not limit the plasticity of the film, therefore the dislocation velocities do not play a crucial role in delaying the relaxation. The difference observed between the critical thicknesses 0.8 and 1.2 μm found respectively for slow and fast cooling rates may be ascribed to the fact that the slow rate keeps the sample at a high temperature for a longer time than does the fast one. The growth parameters were the following:

(i) for the slow cooled samples, the 0.8 μm thick layer was deposited at 750 °C for 10 min and the cooling step (between 750 and 600 °C) was as long as 30 min;
(ii) for the fast cooled samples, the 1.2 μm thick layer was deposited at 750 °C for 15 min and the cooling step (between 750 and 600 °C) was as short as 3 min.

As the dislocation configurations are similar in both cases (onset of relaxation) one can assume that the overall thermal effects (growing plus cooling step) are the same.

The frequent occurrence of blocking interactions observed between a threading segment and an already developed misfit dislocation seems contradictory with the fact that the film thickness t_F is considerably higher than the critical one. For GaAs/Ge with a misfit $m = 7.2 \times 10^{-4}$, the resolved mismatch stress is

$$\sigma = s\frac{E}{1-\nu}m \approx 50 \text{ MPa} \tag{1}$$

with s the Schmidt factor, E the Young modulus and ν the Poisson ratio. If we consider the distance z^* (figure 6) over which the background mismatch stress is negated by the misfit dislocation, using the simple expression $\sigma = \mu b/2\pi z$ for the stress at a distance z from that dislocation one obtains $z^* < 0.1$ μm. Thus the GaAs layers always corresponded to $t - z^* > t_c$, i.e. the condition for which in the Freund model [11] there should not be any impediment in the threading segment movement, but in which we actually observed blocking situations.

It is usually assumed in the concept of critical thickness that the whole threading dislocation segment is lying in a glide plane, i.e. the glissile dislocation length is equal to the length of

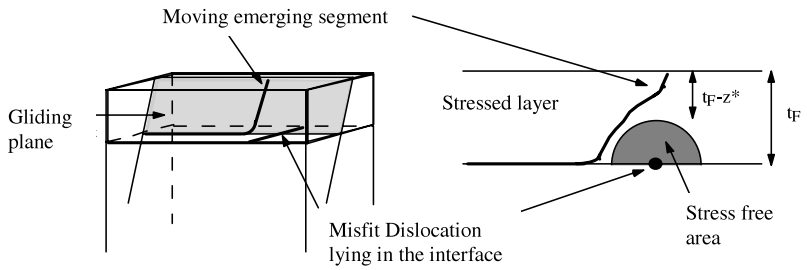

Figure 6. Illustration of the blocking interaction in the model by Freund [11].

the (111) plane principal line through the whole film. However, these threading segments (TDs) are produced during the growth by replication of dislocations from the substrate, so they would lie in no special geometry. They will glide only if at least a part of the TD is elongated into a (111) glide plane. Of course the dislocation segment could orient itself within a $\{111\}$ plane during the growth but the complete achievement of this depends on the growth rate. So we suggest that during the film growth, the threading dislocation with no special orientation should be moved partially in a $\{111\}$ plane, as suggested by Strunk *et al* [14] in the Ge/GaAs system; in such a case the critical length value calculated by Matthews must be compared to the effective length in the $\{111\}$ plane, and not to the layer thickness or its projection along the $\{111\}$ principal line.

The surprisingly low dislocation velocities we measured in the films during post-growth annealing at 430 °C, as compared to bulk experiments, may be ascribed to the fact that, if the dislocation length is shorter than the distance between two double kinks (DKs), the velocity is proportional to that length [15]; so very low dislocation velocities can be obtained for very short lengths.

In GaAs the variation of the DK distance with temperature is not precisely known, but it can be estimated to be between a few tenths of a micron and a few microns at medium temperatures [16]. So these low dislocation velocities could be explained if the moving segment length is shorter than the DK distance.

These remarks bring us to the fact that the Matthews model applied to the film thickness is not a suitable criterion to explain the previous results in GaAs/Ge and probably in other systems relaxing in the same way; the relaxation would not be directly related to the film critical thickness but rather to a critical length L_c of a part of the TD lying in a (111) plane. The movement of the as-grown TD, being in no special orientation, in a (111) plane depends on climbing events: therefore it is thermally activated.

So using the same arguments as Matthews and Blakeslee [2], one can obtain a critical glissile length L_c of 0.24 μm (table 1), assuming that, whatever the film thickness, the observation of the first MD (figure 1) corresponds to this length. One can also explain that

(i) the same critical length may be obtained with different film thicknesses (and different cooling rates) provided the overall thermal effects are similar;
(ii) the interactions between a threading segment and an MD already developed often give a blocking situation because, as the free glissile length is just above L_c, the opposing stress of a previously developed MD impedes the moving TD;
(iii) the very limited dislocation displacements observed at 430 °C are coherent with the length-proportional velocity regime, assuming the glissile length of the moving dislocation is as short as $\approx$0.3 μm (the transition between both regimes is expected to occur above 3 μm [16]).

Thus assuming that the relaxation-delaying mechanism is the climbing of part of a TD up to (111) planes, to obtain the same thermal effect in slow and fast cooling, the threading segment (figure 7) should receive the same number of point defects per unit length. During time t at a temperature T, the point defects, which diffuse toward the dislocation, are contained in a cylinder, the axis of which is the dislocation, and with a radius $\ell = \sqrt{Dt}$ where D is the point defect diffusion coefficient. The number of point defects reaching the dislocation during time t per unit length is thus

$$\pi \ell^2 C = \pi DCt = At \exp(-Q/kT) \tag{2}$$

where C is the point defect concentration, A a constant and Q the activation energy of the thermally activated process. (On cooling the previous equation should be integrated over the temperature ramp.)

Assuming that the number of point defects is the same in both cooling treatments, since it corresponds to the onset of the relaxation (same critical length), allows us to determine Q as equal to 2.9 eV. This value is very close to the self-diffusion activation energy for GaAs measured by radiotracers, ranging between 2.6 and 3.2 eV with similar values for Ga or As atoms [17, 18]. This strongly sustains the existence of a critical length of TD rather than a critical thickness for MD production, only a part of the TD being glissile.

3.2. Dislocation cross-slip

Some authors have observed cross-slip and uncommon glide systems already [19, 20] similarly to what we reported in section 2. Especially, Albrecht *et al* [19] developed a mechanical equilibrium analysis that includes a frictional force on the gliding dislocations and showed that further secondary glide planes such as $\{101\}$ and $\{131\}$ could occur in semiconductors with diamond or zinc-blende structures but in rather higher misfit systems.

As regards the resolved stress and the dissociated dislocations, two conditions are required for dislocation cross-slipping:

(i) the resolved shear stress in the new glide plane must be greater than or equal to the one in the primary plane, at least locally;
(ii) the cross-slip is only possible if the partial dislocations are locally shrunk and in screw orientation [23].

3.2.1. Cross-slip in $\{111\}$ planes. In fourfold symmetry epitaxial films, all the $(a/2)\langle 110\rangle\{111\}$ systems experience the same resolved shear stress: the first condition is thus always fulfilled for $\{111\}$ glide. Considering shrinkage of the stacking fault ribbon, a moving dissociated emerging segment in a $\{111\}$ plane experiences a differential effect of the stress on both threading partials which reduces the dissociation width and favours the cross-slip in 50% of the cases, i.e. when the leading partial is the slowest. Moreover, for a threading dissociated dislocation blocked against an obstacle, this shrinking effect may become more pronounced. If the leading partial is blocked, the stress pushes the trailing partial that allows the stacking fault ribbon to be shrunk. The equilibrium dissociation width r_e can then be calculated as a function of the misfit m [9]; for example when the 60° segment is the leading partial this gives

$$r_e = \frac{\mu a^2}{24\pi} \frac{1}{\gamma + \frac{aE}{3\sqrt{3}(1-\nu)} m} \tag{3}$$

with a the lattice parameter, γ the stacking fault energy and μ the shear modulus of the film. This provides a very sharp decrease in the dissociation width (with $\gamma = 60$ mJ m^{-2} [24]) when

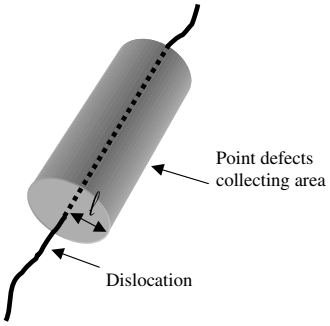

Figure 7. Point defect flux towards a dislocation.

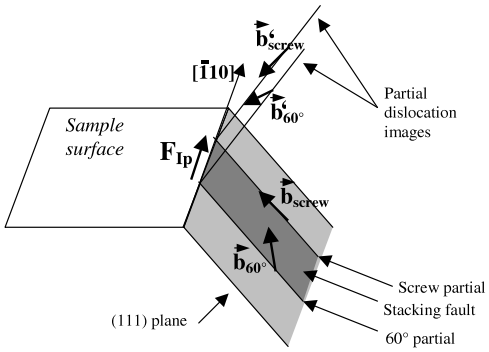

Figure 8. Partial dislocations and their images in the (111) plane. F_{Ip} is the projection of the image force acting on the 60° partial along the [110] direction.

the misfit is increased: cross-slip events thus become very easy above 1% misfit. However, in our samples, we observe cross-slip and multiple cross-slip events for misfit levels lower than 0.1%: this shrinkage effect is therefore not sufficient to explain our observations.

The parts of the threading dislocations emerging at the very surface and their interaction with the sample surface are probably involved in this very easy cross-slip process: as the $\{111\}$ planes are not normal to the surface, the emerging segment with its image makes an angular dislocation; if we consider a dissociated emerging segment along the principal line $[11\bar{2}]$ in the (111) plane (figure 8), one can calculate the image force that acts on both partial dislocations (60° and screw) [25].

For this calculation, we used the stress field of a dislocation which meets the free surface of a semi-infinite isotropic solid, given by Shaibani and Hazzledine [26]. The total stress tensor depends on various parameters, such as the angle φ between the glide plane and the sample surface, the shear modulus and Poisson ratio, and it is defined at any point $M(x, y, z)$ below the free surface. The effect of the interaction between the emerging segment and its image dislocation is contained in the line tension effect that reduces the dislocation length. The image force is thus higher when the angle φ is smaller.

Using the Peach–Koehler relationship, this stress field allows us to calculate the force F_{Ip} due to the image dislocation that acts on the trailing partial, in the $[\bar{1}10]$ direction, when the leading one is supposed to be blocked against an obstacle as considered previously. If the trailing is the screw partial, these calculations show that F_{Ip} is equal to zero: this means that the image force does not affect the equilibrium dissociation width calculated from equation (1).

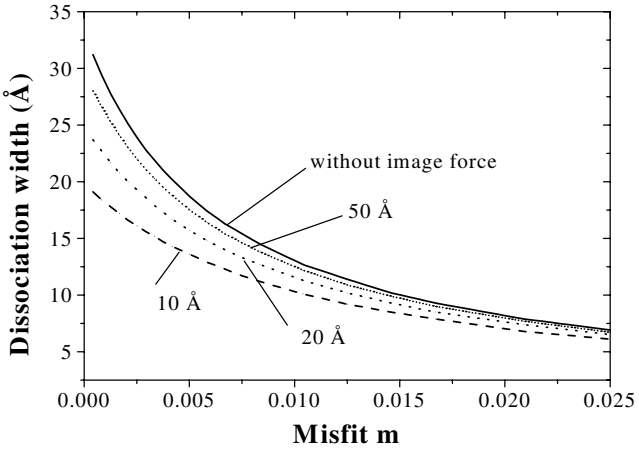

Figure 9. Equilibrium dissociation width r_e as a function of the lattice mismatch in the $Si_{1-x}Ge_x$/Si system when the 60° is the trailing partial; r_e is calculated from equation (4) at different depths from the surface: 10, 20, 50 Å.

In contrast, the image force that acts on the 60° partial along the $[\bar{1}10]$ direction is not equal to zero: this force has therefore to be taken into account in the equilibrium dissociation width calculation, when the 60° partial is the trailing partial. Thus, equation (3) becomes

$$r_e = \frac{\mu a^2}{24\pi} \frac{1}{\gamma + \frac{aE}{6\sqrt{3}(1-\nu)} m + F_{Ip}} \tag{4}$$

(the force due to the biaxial stress in the layer is half that in equation (1) because the trailing partial is the 60°).

Figure 9 shows, in the case of the SiGe/Si system, the equilibrium dissociation width according to the lattice mismatch m, and calculated at different positions from the free surface (the same value of γ as above). It is clear that the fault shrinkage is favoured by the image force near the free surface; this effect is significant only for distances lower than 20 Å from the free surface, thus leading to a very local shrinkage of the fault ribbon. Finally, one can see in figure 9 that the effect of the image force is more pronounced for lattice mismatches lower than 1%.

These results are in agreement with the observations and calculations of Hazzledine and co-workers [27] who showed that the dissociation width could be greatly changed near a free surface.

The image force is thus important at the surface of the sample, and can act to locally shrink the fault ribbon. Then, the line tension which tends to reduce the dislocation length allows the emerging segment to move out of its glide plane, at least locally (near the surface). Both effects help the emerging segment to cross-slip when it is blocked against an obstacle. This mechanism is shown in figure 10: considering an emerging segment blocked against an obstacle in the (111) plane, the image force produces a local shrinkage of the emerging segment and allows it to glide in another plane; then, the force due to the lattice mismatch (F_m) allows the dislocation to develop in this new glide plane, the shrinkage gliding along the intersection of the two glide planes. Whatever the {111} planes, the angles with the (001) sample surface are the same: all the 60° emerging segments experience the same image force. The resolved shear stress is the same in all {111} planes as well. Both forces (the image force and the one due to the stress in the film) favour the glide plane change every time the emerging segment

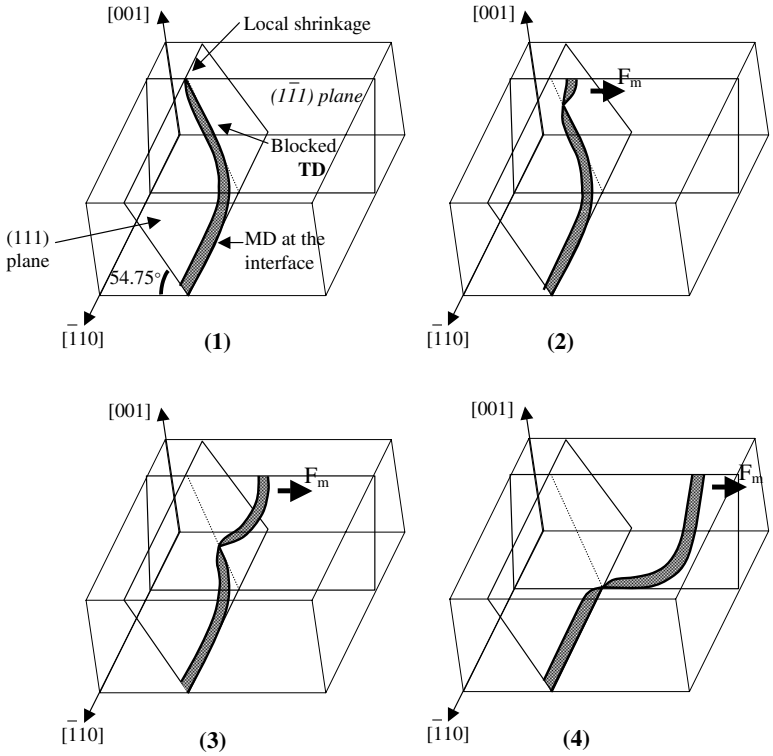

Figure 10. Four steps of the cross-slip process in the {111} planes. The initial shrinkage at the surface glides along the intersection between the two glide planes. F_m is the force exerted on the TD due to the lattice mismatch.

Table 2. Schmidt factors in the different glide planes for an MD with Burgers vector $(a/2)[101]$; ϕ is the angle between the glide plane normal and the growth direction.

Glide plane	(111)	(101)	(131)
Interface MD slip trace	$[\bar{1}10]$	[010]	$[3\bar{1}0]$
Schmidt factor	0.41	0.5	0.21
ϕ (deg)	54.7	45	72.5

is blocked by an obstacle, allowing cross-slip and multiple cross-slip events to occur easily using ⟨110⟩ interfacial directions.

3.2.2. Cross-slip in {101} and {131} planes. In the case of these uncommon glide systems, the resolved shear stress on misfit dislocations is different according to the glide plane, as illustrated in table 2 by the Schmidt factor for an $(a/2)[\bar{1}01]$ glide dislocation. The resolved shear stress is higher in the {101} plane than in the {111} plane, but lower when the cross-slip takes place in the {131} plane. The first condition (i) for the cross-slip is thus not fulfilled in this second case, at least in the absence of local stress enhancement due to dislocation interaction.

The reduction of the dissociation width due to image forces allowing the emerging segment to slip out of its primary glide plane cannot be calculated because the dislocation dissociation

characteristics in the {101} and {131} planes are not exactly known. These characteristics cannot be determined experimentally either, because XRT has too low resolution and the dislocation density is too small for TEM to be performed.

The image force depends on the angle ϕ between the growth direction [001] (normal to the sample surface) and the glide plane normal. This angle is respectively equal to 45°, 54.7° and 72.5° for the {101}, {111} and {131} planes. The image force is thus the highest in the {101} planes, and the lowest in the {131} planes.

The high value of the resolved shear stress in the {101} plane, together with the shrinkage effect in the primary {111} plane due to the image force, can be responsible for cross-slip in these planes; however, as the image force is high in these planes, the emerging segment is not in a stable configuration, and a new cross-slip in a {111} plane is favoured as soon as the dislocation is blocked.

In {131} planes, the lower value of the image force allows the emerging segment to be in a more stable configuration, and can thus explain the cross-slip in these planes, insofar as the emerging segment is blocked and locally shrunk in the primary {111} plane; however, as the stress level is low in these planes, the dislocation may rapidly change its glide plane and return in a {111} plane when meeting an obstacle.

Both the resolved shear stress and the image force have thus to be taken into account in these uncommon cross-slip events. Finally, the effect of temperature could also favour an uncommon glide system: actually, cross-slip in {101} and {131} planes has been observed in GaAs layers with a growth temperature close to the end of the thermally activated yielding regime.

4. Conclusion

A very high metastability was obtained in low misfit heteroepitaxial systems, the very first MD appearing far above the Matthews critical thickness. The influence of the cooling rate was also noticed in the GaAs/Ge system which can be interpreted in terms of equivalent overall thermal effects. In addition, frequent blocking interactions similar to those proposed by Freund [11] were observed whereas the conditions for these interactions were, in principle, not fulfilled. Finally unusual low threading dislocation velocities were measured during further heat treatments around 400 °C. All these results may be interpreted by considering that the concept of critical thickness should be replaced by a critical length of threading dislocation lying in the (111) glide plane. As the length of a TD in a glide plane is larger than this critical length (which can be calculated using the same arguments as Matthews and Blakeslee [2]), the TD can move driving the MD development independently of the film thickness. We proposed the climbing of part of a TD up to (111) planes as the relaxation-delaying mechanism which obviously depends on point defect fluxes toward dislocations. Of course, everything which helps the dislocation to climb will promote the relaxation: high temperature growth, high temperature annealing, high misfit stresses promoting point defect super-saturation etc.

As obtained a few years ago in metallic bulk materials [28] observations on strained semiconductor epilayers show evidence of cross-slip and multiple cross-slip events at very low stresses. The cross-slip of MD occurs at the very first stages of plastic relaxation, i.e. for low MD densities ($<10^3$ cm cm^{-2}) and without interaction which could promote this process. Cross-slip events have been observed in the {111} glide planes, in both ⟨110⟩ interface directions, as well as in the uncommon glide planes {101} and {131}.

The parts of the threading dislocations emerging at the very surface and their interaction with the free surface of the samples could be involved in this process: actually, the image

force can act to locally shrink the fault ribbon and allow the emerging segment to slip out of its glide plane. Uncommon cross-slip events have been analysed involving a balance between the effects of both the image force and the resolved shear stress, even if the image force in the $\{101\}$ and $\{131\}$ planes cannot be exactly evaluated as long as the dislocation dissociation characteristics in these planes are not known.

This easy cross-slip is a very important mechanism which allows us to avoid blocking situations between two TDs during their development, favouring the homogenization of the relaxation and its complete achievement.

References

[1] Frank F C and van der Merwe J H 1949 *Proc. R. Soc.* A **198** 205
Frank F C and van der Merwe J H 1949 *Proc. R. Soc.* A **198** 216
Frank F C and van der Merwe J H 1949 *Proc. R. Soc.* A **200** 125
[2] Matthews J W and Blakeslee A E 1974 *J. Cryst. Growth* **27** 118
Matthews J W and Blakeslee A E 1975 *J. Cryst. Growth* **29** 273
Matthews J W and Blakeslee A E 1976 *J. Cryst. Growth* **32** 265
[3] Matthews J W, Mader S and Light T B 1970 *J. Appl. Phys.* **41** 3800
[4] Dodson B W and Tsao J Y 1987 *Appl. Phys. Lett.* **51** 1325
[5] Houghton D C 1991 *J. Appl. Phys.* **70** 2136
[6] Hull R, Bean J C and Buescher C 1989 *J. Appl. Phys.* **66** 5837
[7] Fox B A and Jesser W A 1990 *J. Appl. Phys.* **68** 2801
[8] Perovic D D and Houghton D C 1995 *Inst. Phys. Conf. Ser.* **146** 117
[9] Pichaud B, Putero M and Burle N 1999 *Phys. Status Solidi* a **171** 25
[10] Putero M, Burle N and Pichaud B 1999 *Phil. Mag.* A **79** 2711
[11] Freund L B 1990 *J. Appl. Phys.* **68** 2073
[12] Choi S K, Mihara M and Nimomiya T 1977 *Japan. J. Appl. Phys.* **16** 737
[13] Djemel A and Castaing J 1986 *Europhys. Lett.* **2** 611
[14] Strunk H P, Hagen W and Bauser E 1979 *Appl. Phys.* **18** 67
[15] Hirth J P and Lothe J 1982 *Theory of Dislocations* (New York: Wiley)
[16] Caillard D, Clement N, Couret A, Androussi Y, Lefebvre A and Vanderschaeve G 1987 *Inst. Phys. Conf. Ser.* **87** 361
[17] Kendall D L 1968 *Semiconductors and Semimetals* ed R K Willardson and A C Beer (New York: Academic) p 163
[18] Palfrey H D, Brown M and Willoughby A F W 1981 *J. Electrochem. Soc.* **128** 2224
Palfrey H D, Brown M and Willoughby A F W 1983 *J. Electron. Mater.* **12** 863
[19] Albrecht M, Strunk H P, Hull R and Bonar J M 1993 *Appl. Phys. Lett.* **62** 2206
[20] Ulhaq-Bouillet C, Lefebvre A and Di Persio J 1994 *Phil. Mag.* A **69** 995
[21] Köhler R, Pfeiffer J U, Raidt H, Neumann W, Zaumseil P and Richter R 1998 *Cryst. Res. Technol.* **33** 593
[22] Lacey G, Whitehouse C R, Parbrook P J, Cullis A G, Keir A M, Moeck P, Johnson A D, Smith G W, Clark G F, Tanner B K, Martin T, Lunn B, Hogg J H C, Emeny M T, Murphy B and Bennett S 1998 *Appl. Surf. Sci.* **123/124** 718
[23] Escaig B 1968 *J. Physique* **29** 225
[24] Alexander H 1979 *J. Physique* **C6** 1
[25] Putero M, Burle N and Pichaud B 2001 *Phil. Mag.* A **81** 125
[26] Shaibani S J and Hazzledine P M 1981 *Phil. Mag.* A **44** 657
[27] Hazzledine P M, Karnthaler H P and Wintner E 1975 *Phil. Mag.* **32** 81
[28] Pichaud B and Minari F 1976 *Phil. Mag.* **34** 1121